Enhancement of optical nonlinearity through shape distribution

2001 J. Phys.: Condens. Matter 13 7271

(http://iopscience.iop.org/0953-8984/13/33/308)

INSTITUTE OF PHYSICS PUBLISHING JOURNAL OF PHYSICS: CONDENSED MATTER

J. Phys.: Condens. Matter **13** (2001) 7271–7282 PII: S0953-8984(01)23863-6

Enhancement of optical nonlinearity through shape distribution

L Gao[1,2,3], Z Y Li[1,2] and K W Yu[4]

[1] CCAST (World Laboratory), PO Box 8730, Beijing 100080, China
[2] Department of Physics, Suzhou University, Suzhou 215006, China
[3] Laboratory of Solid State Microstructures, Nanjing University, Nanjing 210008, China
[4] Department of Physics, Chinese University of Hong Kong, Shatin, New Territories, Hong Kong, China

Received 11 April 2001, in final form 4 July 2001
Published 2 August 2001
Online at stacks.iop.org/JPhysCM/13/7271

Abstract

The effect of the shape distribution of granular inclusions on the effective nonlinear optical properties of granular metal/dielectric composites is considered. The study is based on a generalized Maxwell–Garnett type approximation for the spectral density function of two-component composites in which the metallic inclusions possess a 'beta function' distribution of geometric shapes. Numerical results show that the spectral density function is increased (decreased) in the range $0.35 \leqslant s' \leqslant 0.5$ ($0.8 \leqslant s' \leqslant 1.0$) with increasing shape distribution parameter α. By invoking the mean-field approximation, we calculate the optical nonlinearity and find the nonlinearity enhancement peak is separated from the absorption peak in the range $0.45 \leqslant \omega/\omega_p \leqslant 0.6$, while a large enhancement of the optical nonlinearity is found in the range $0.8 \leqslant \omega/\omega_p \leqslant 1.0$. Thus by introducing a shape distribution of metallic particles, we are able to make the figure of merit attractive in this frequency range. In the dilute limit, the shape distribution leads to an anomalous far-infrared optical absorption. Moreover, an exact formula for the effective optical nonlinearity is derived and a sharp nonlinearity enhancement peak is observed near the resonant frequency $\omega/\omega_p \approx 0.47$.

1. Introduction

Nonlinear optical properties of granular composite materials have attracted much interest in physics and engineering [1, 2]. A typical system for the theoretical and experimental investigations is composed of metallic particles with nonlinear dielectric response, randomly embedded in a dielectric host with linear or nonlinear response. Such a composite system exhibits strong nonlinear optical susceptibility through the local field and geometric resonance effects [3–7]. We also know that composites of small metallic particles possess anomalous far-infrared absorption [8]. Both the optical absorption and optical nonlinearity are strongly dependent on the composite microgeometry [3–7, 9–11].

In recent works [10, 11], we have investigated the effect of particle shape on the nonlinear optical susceptibility of metal/dielectric composite media. The results show that both the magnitude and the position of nonlinearity enhancement can be adjusted by the use of non-spherical inclusions. Furthermore, the frequency at which the nonlinearity enhancement peak occurs, is the same as the one for optical absorption peak. This hinders the applicability of such composites, as for practical applications, the most useful parameter is the figure of merit, which is proportional to the optical nonlinearity, and inversely proportional to the optical absorption [12]. In this regard, we can manipulate anisotropic [4, 6] and correlated [13] microstructures to achieve a large enhancement of optical nonlinearity and a concomitant suppression of optical absorption.

In the work [11], we derived Maxwell–Garnett type approximations to investigate the depolarization factor on the effective dielectric response based on the assumption that all the metallic particles have the same shape and depolarization factor. However, according to the analysis of the absorption coefficient and conjugate reflectivity in related experiments, it has been shown that the particles have a shape distribution. In this paper, we study a composite metal/dielectric system of spheroidal particles with a distribution of particle shape. Bohren and Huffman [14] suggested that spectra of particles of any complicated form may be approximated by the average spectra of spheroidal particles. The case of spheroidal particles enables one to consider a broad spectrum of inclusions from sharp needles to flat discs. We assume here that the shape distribution has the 'beta function' form [15]. Such an assumption is not accidental. Recently, Zakri *et al* [16] verified that the 'beta function' distribution could lead to the famous Lichtenecker formulae [17]. Moreover, this form allows us an alternative freedom, i.e., the distribution parameter α, of adjusting the magnitude of the optical absorption and nonlinearity enhancement. We directly generalize the Maxwell–Garnett type approximation to investigate the system in which an assembly of small spheroidal particles have the 'beta function' shape distribution through the spectral representation [18, 19]. In the dilute limit, an expression for the optical nonlinearity is derived from the definition for the first time.

Our paper is organized as follows. In section 2, we derive the Maxwell–Garnett approximation by taking the shape distribution into account and the spectral density function is solved both numerically and analytically for different distribution parameters. With the spectral function, we study the optical absorption, optical nonlinearity enhancement and the figure of merit in section 3. In section 4, we investigate the dilute case and derive an analytical expression for the effective optical nonlinearity. A summary of our results and a discussion is given in section 5.

2. Maxwell–Garnett type approximation with shape distribution

We firstly consider a nonlinear composite system in which randomly oriented, spheroidal particles of volume fraction f are embedded in an isotropic dielectric host medium of volume fraction $1 - f$. The local constitutive $\boldsymbol{D}$–$\boldsymbol{E}$ relation of components is characterized by the weakly-nonlinear form $\boldsymbol{D} = \epsilon_i^{(0)}\boldsymbol{E} + \chi_i^{(3)}|\boldsymbol{E}|^2\boldsymbol{E}$, where $\epsilon_i^{(0)}$ and $\chi_i^{(3)}$ are the (scalar) dielectric constant and the third-order nonlinear optical susceptibility (optical nonlinearity) of the ith component. Throughout the work, the magnitude of the nonlinear term $\chi_i^{(3)}|\boldsymbol{E}|^2$ is assumed to be weak, i.e., it is smaller than that of the linear part $\epsilon_i^{(0)}$. The same assumption has been already made and such cubic nonlinearity is the lowest-order nonlinearity appearing in a material with inversion symmetry [3–7, 9–11]. The spheroidal particles are described by two depolarization factors L_z and L_{xy}, which satisfy $L_z + 2L_{xy} = 1$. In this notion, For

spherical particles, $L_z = L_{xy} = 1/3$, while for needle-like ones, $L_z \approx 0$ and $L_{xy} \approx 1/2$ and for platelike ones $L_{xy} \approx 0$, $L_z \approx 1$.

We apply the electric field $\boldsymbol{E}_0$ along the z-axis, and take the principal axis of spheroidal particles to be oriented at any angle θ to the axis. Since the uniaxial axis of the spheroidal particles is assumed to be randomly oriented in space, the effective response will still be isotropic. We calculate the average electric field in the spheroidal inclusions

$$\langle \boldsymbol{E}_1 \rangle = \frac{1}{3}\left[\frac{\epsilon_2^{(0)}}{L_z\epsilon_1^{(0)} + (1-L_z)\epsilon_2^{(0)}} + \frac{2\epsilon_2^{(0)}}{L_{xy}\epsilon_1^{(0)} + (1-L_{xy})\epsilon_2^{(0)}}\right]\langle \boldsymbol{E}_L \rangle \tag{1}$$

where the Lorentz local field $\langle \boldsymbol{E}_L \rangle$ includes the contribution from the dipole moments of all other inclusions. The expressions for the spatial average of the electric field $\langle \boldsymbol{E} \rangle$ and displacement $\langle \boldsymbol{D} \rangle$ are, respectively,

$$\langle \boldsymbol{E} \rangle = \boldsymbol{E}_0 = f\langle \boldsymbol{E}_1 \rangle + (1-f)\langle \boldsymbol{E}_L \rangle \tag{2}$$

and

$$\langle \boldsymbol{D} \rangle = f\epsilon_1^{(0)}\langle \boldsymbol{E}_1 \rangle + (1-f)\epsilon_2^{(0)}\langle \boldsymbol{E}_L \rangle. \tag{3}$$

According to the definition, the effective linear dielectric function $\epsilon_e^{(0)}$ is then given as follows:

$$\epsilon_e^{(0)} = \frac{\langle \boldsymbol{D} \rangle}{\langle \boldsymbol{E} \rangle} = \frac{f\epsilon_1^{(0)}\langle \boldsymbol{E}_1 \rangle + (1-f)\epsilon_2^{(0)}\langle \boldsymbol{E}_L \rangle}{f\langle \boldsymbol{E}_1 \rangle + (1-f)\langle \boldsymbol{E}_L \rangle} = \frac{f\epsilon_1^{(0)}\beta + (1-f)\epsilon_2^{(0)}}{f\beta + 1 - f} \tag{4}$$

where the field factor $\beta \equiv \langle \boldsymbol{E}_1 \rangle / \langle \boldsymbol{E}_L \rangle$. As mutipole interaction between different polarizations is explicitly neglected during the derivation, equation (4) is only suitable for not very large volume fractions [11, 20].

For an assembly of metal particles having different spheroidal shapes, the field factor has the form

$$\beta = \frac{1}{3}\int \left[\frac{\epsilon_2^{(0)}}{\epsilon_2^{(0)} + L_z\left(\epsilon_1^{(0)} - \epsilon_2^{(0)}\right)} + \frac{2\epsilon_2^{(0)}}{\epsilon_2^{(0)} + L_{xy}\left(\epsilon_1^{(0)} - \epsilon_2^{(0)}\right)}\right] P(L_z)\,\mathrm{d}L_z \tag{5}$$

where $P(L_z)$ is the shape distribution of the spheroidal particles; in other words, $P(L_z)\,\mathrm{d}L_z$ is the probability for a spheroid to have the depolarization factor L_z lying within the interval $(L_z, L_z + \mathrm{d}L_z)$. The distribution function must be chosen so as to satisfy $\int_0^1 P(L_z)\,\mathrm{d}L_z = 1$.

Here, we make the assumption that $P(L_z)$ has 'beta function' form and is expressed through the Γ-function [15, 16],

$$P_\alpha(L_z) = \frac{\Gamma(2)}{\Gamma(1-\alpha)\Gamma(1+\alpha)} L_z^{-\alpha}(1-L_z)^\alpha \qquad -1 \leqslant \alpha \leqslant 1 \tag{6}$$

where α is the distribution parameter and Γ is the gamma function. The distribution function has special properties such as $P_1(L_z) = \delta(L_z)$, $P_{-1}(L_z) = \delta(1-L_z)$ and $P_0(L_z) = 1$ (corresponding to the uniform distribution). An alternative distribution such as the log-normal form [21] can be introduced in a similar way.

If $\alpha \neq 0$, after a tedious calculation, we have

$$\beta = \frac{1}{3\alpha(1-r)}\left[\frac{2^{\alpha+2}}{(1+r)^\alpha} - 3 - r^\alpha\right] \tag{7}$$

where $r \equiv \epsilon_1^{(0)}/\epsilon_2^{(0)}$ is the dielectric contrast between metal particles and the dielectric host. Substituting equation (7) into (5) leads to the following equation:

$$\frac{\epsilon_e^{(0)}}{\epsilon_2^{(0)}} = \frac{f[2^{\alpha+2} - (3+r^\alpha)(1+r)^\alpha]r + 3(1-f)\alpha(1-r)(1+r)^\alpha}{f[2^{\alpha+2} - (3+r^\alpha)(1+r)^\alpha] + 3(1-f)\alpha(1-r)(1+r)^\alpha}. \tag{8}$$

If $\alpha = 0$, the field factor is then simplified as

$$\beta = \frac{1}{3(1-r)} \ln \left[\left(\frac{2}{1+r} \right)^4 \Big/ r \right]. \tag{9}$$

Similarly, the effective linear dielectric function can be obtained by introducing equation (9) into equation (5),

$$\frac{\epsilon_e^{(0)}}{\epsilon_2^{(0)}} = \frac{fr \ln \left[\left(\frac{2}{1+r} \right)^4 \Big/ r \right] + 3(1-r)(1-f)}{f \ln \left[\left(\frac{2}{1+r} \right)^4 \Big/ r \right] + 3(1-r)(1-f)}. \tag{10}$$

Next, we adopt the spectral representation [18, 19], which is convenient for two-component composites, to calculate the effective linear dielectric function and optical nonlinearity. The key parameter in the spectral representation is the spectral density function $m(s')$, which is obtained through the limiting process

$$m(s') = \lim_{\eta \to 0^+} -\frac{1}{\pi} \mathrm{Im}[F(s' + \mathrm{i}\eta)] \tag{11}$$

where $F(s) \equiv 1 - \epsilon_e^{(0)}/\epsilon_2^{(0)} = \int_0^1 [m(s')/(s - s')]\, \mathrm{d}s'$ and $s \equiv \epsilon_2^{(0)}/(\epsilon_2^{(0)} - \epsilon_1^{(0)})$.

For $\alpha = 1$, $F(s)$ has the form from equation (7),

$$F(s) = \frac{F_1}{s - s_1} + \frac{F_2}{s - s_2} \tag{12}$$

where the pole $s_1 = 0$ and $s_2 = (3 + 2f)/6$, while the residues F_1 and F_2 are given by

$$F_1 = \frac{f}{3 - 2f} \qquad \text{and} \qquad F_2 = \frac{2(f - f^2)}{3 - 2f}. \tag{13}$$

It is easy to check the sum rule $F_1 + F_2 = 1$. Thus the spectral density function can be written as a sum of two δ-functions by using equation (11),

$$m(s') = F_1 \delta(s' - s_1) + F_2 \delta(s' - s_2). \tag{14}$$

For $\alpha = -1$, we have

$$F(s) = \frac{\frac{2f}{3-f}}{s} + \frac{\frac{f(1-f)}{3-f}}{s - \frac{3-f}{3}} \tag{15}$$

and

$$m(s') = \frac{2f}{3-f} \delta(s') + \frac{f(1-f)}{3-f} \delta \left(s' - \frac{3-f}{3} \right). \tag{16}$$

Again the residues satisfy the sum rule.

For the general case $-1 < \alpha < 1$, the explicit spectral density function may exist [22], but here we resort to numerical solutions. We calculate $m(s')$ numerically from equations (8), (10) and (11) by putting $s = s' + \mathrm{i}\eta$ and choosing the real part at 1000 equally spaced values across the interval $0 < s' < 1$ and η at a small value such as $\eta = 0.001$. The actual value of η is indeed unimportant. We find the choice yields acceptable results by numerically checking the sum rule

$$\int_0^1 m(s')\, \mathrm{d}s' = f. \tag{17}$$

In figure 1, we plot the spectral density function $m(s')$ for various distribution parameters α and volume fractions f. As one can see, the spectrum is continuous from $s' = 0$ to $s' = 1$,

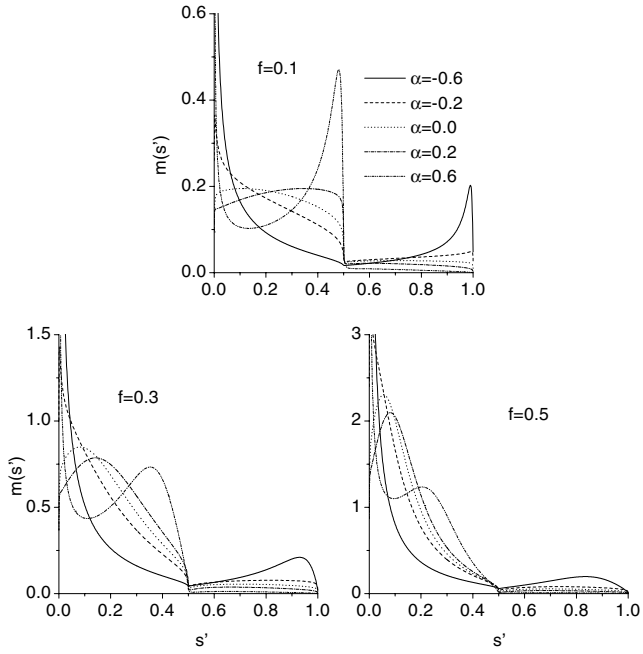

Figure 1. The spectral density $m(s')$ against s' for various volume fractions f and distribution parameters α.

instead of two single δ peaks for the system of spheroidal particles with the same depolarization factors [11]. For $\alpha \to -1$ ($L_z \to 1$), more chainlike isolated clusters are formed, leading to a narrow peak in the middle region $0.35 \leqslant s' \leqslant 0.5$. Moreover, with increasing α, the spectrum in this region is increased monotonically, while it is decreased in the large-s' region $0.8 \leqslant s' \leqslant 1.0$. As we introduce the shape distribution into consideration, the metallic nanoparticles can form larger clusters than for the system without shape distribution [11] even for small f. This is demonstrated by the fact that there are large spectral values at small s'. We indicate that the distribution parameter α, determines the microstructure of the metal components, in its turn, plays an important role in determining the spectral function and will have a further effect on the optical absorption and nonlinearity enhancement. As far as the volume fraction is concerned, with increasing f, the position of the spectral maximum shifts to small s', and the magnitude becomes large, in order to satisfy equation (17). We also numerically calculate the spectra for $\alpha = -1$ and $\alpha = 1$ with equation (4), equation (7) and equation (11). It is found that the behaviour of the curves coincides with that given by equation (14) and equation (16).

3. Optical absorption, optical nonlinearity and figure of merit

As the spectral density function has been numerically or analytically calculated as a function of s' and α, the effective linear dielectric function is represented as

$$\epsilon_e^{(0)} = \epsilon_2^{(0)} \left[1 - \int \frac{m(s')}{s - s'} \, \mathrm{d}s' \right]. \tag{18}$$

Other relevant physical parameters such as the averages of the local fields can also be expressed in terms of the spectral density function,

$$f\langle \boldsymbol{E}^2\rangle_{lin,1} = \int_0^1 \mathrm{d}s' \frac{s^2 m(s')}{(s-s')^2}\boldsymbol{E}_0^2$$
$$(1-f)\langle \boldsymbol{E}^2\rangle_{lin,2} = \left[1 - \int_0^1 \mathrm{d}s' \frac{(s^2-s')m(s')}{(s-s')^2}\right]\boldsymbol{E}_0^2 \tag{19}$$

and

$$f\langle |\boldsymbol{E}|^2\rangle_{lin,1} = \int_0^1 ds' \frac{|s|^2 m(s')}{|s-s'|^2}\boldsymbol{E}_0^2$$
$$(1-f)\langle |\boldsymbol{E}|^2\rangle_{lin,2} = \left[1 - \int_0^1 \mathrm{d}s' \frac{(|s|^2-s')m(s')}{|s-s'|^2}\right]\boldsymbol{E}_0^2. \tag{20}$$

As the magnitude of the nonlinear term is usually small, the problem for solving the effective nonlinear susceptibility $\chi_e^{(3)}$ can be treated in the perturbation sense and $\chi_e^{(3)}$ is then evaluated from the linear local fields,

$$\chi_e^{(3)}|\boldsymbol{E}_0|^2\boldsymbol{E}_0^2 = f\chi_1^{(3)}\langle |\boldsymbol{E}|^2\boldsymbol{E}^2\rangle_{lin,1} + (1-f)\chi_2^{(3)}\langle |\boldsymbol{E}|^2\boldsymbol{E}^2\rangle_{lin,2}$$
$$\approx f\chi_1^{(3)}\langle |\boldsymbol{E}|^2\rangle_{lin,1}\langle \boldsymbol{E}^2\rangle_{lin,1} + (1-f)\chi_2^{(3)}\langle |\boldsymbol{E}|^2\rangle_{lin,2}\langle \boldsymbol{E}^2\rangle_{lin,2}. \tag{21}$$

Equation (21) can be applicable to weak nonlinearity and the last equality results from the mean-field approximation, which holds well when the local electric field insides the components is a constant and becomes rough when the fluctuation of the local field is large. For strong nonlinear composite media, we refer the reader to [23].

Next we describe the dielectric function of the metal particles and the host medium. We adopt the Drude model for $\epsilon_1^{(0)}$,

$$\epsilon_1^{(0)} = 1 - \frac{\omega_p^2}{\omega(\omega + \mathrm{i}\gamma)} \tag{22}$$

where ω_p is the plasmon frequency and γ is the damping constant. For numerical calculation, we choose $\gamma = 0.01\omega_p$, which is typical of a good bulk metal, and $\epsilon_2^{(0)} = 1.77$, which is the dielectric constant of water. More recent observations in experiments [24] imply that $\chi_2^{(3)}$ of the dielectric matrix is about several orders magnitude ($\sim 10^7$) less than $\chi_1^{(3)}$ of metallic particles and the dielectric matrix to $\chi_e^{(3)}$ can be negligible. Thus it is reasonable to assume metallic components to be nonlinear, i.e., $\chi_2^{(3)} = 0$. Here we should mention that equation (21) can nevertheless be applicable to the composite media in which both metallic and dielectric components have nonlinear dielectric responses.

In figures 2(a) and (b) the optical absorption spectrum, which is defined as the imaginary part of the effective linear dielectric function $\mathrm{Im}(\epsilon_e^{(0)})$, is plotted versus the frequency ω/ω_p for various values of α. As is evident from the results, the behaviour of optical absorption spectra is quite similar to that of the spectral density function. Concretely speaking, with increasing α, they take on a monotonic increase in the middle-frequency region $0.45 \leqslant \omega/\omega_p \leqslant 0.6$, but a monotonic decrease in the large-frequency region $0.8 \leqslant \omega/\omega_p \leqslant 1.0$. Since the shape of spheroidal particles has a kind of distribution, the surface plasmon resonance peak predicted in [11] will broaden, accompanied by a red-shift, resulting in large optical absorption in the far-infrared region. As f increases, the maximum of the surface plasmon resonance bands exhibits a red-shift too. For $\alpha = -1$ (or $\alpha = 1$), this corresponds to the case where L_z takes only one value, units 1 (or zero). Therefore, the optical absorptions shown in figure 2(b) are the same as the results in previous work [11].

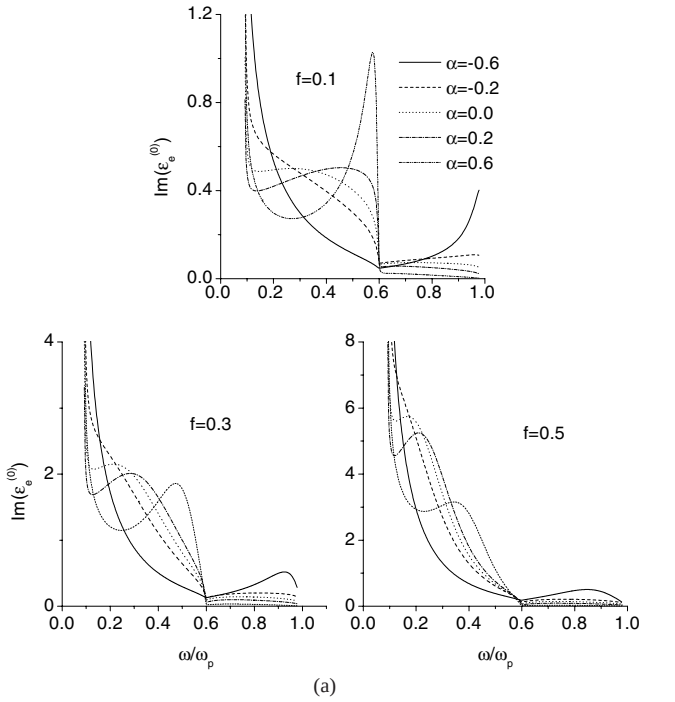

(a)

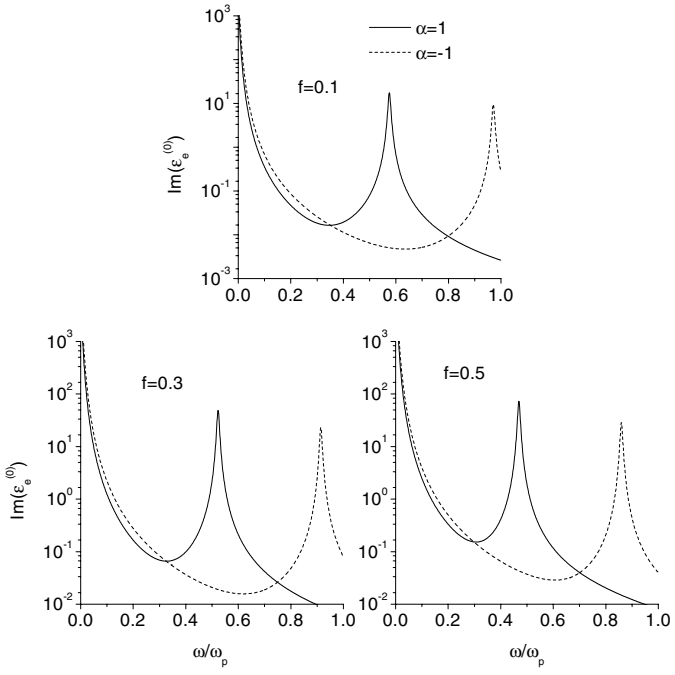

(b)

Figure 2. The optical absorption $\mathrm{Im}(\epsilon_e^{(0)})$ against the frequency ω/ω_p for various f and α, as shown in 2(a) and 2(b).

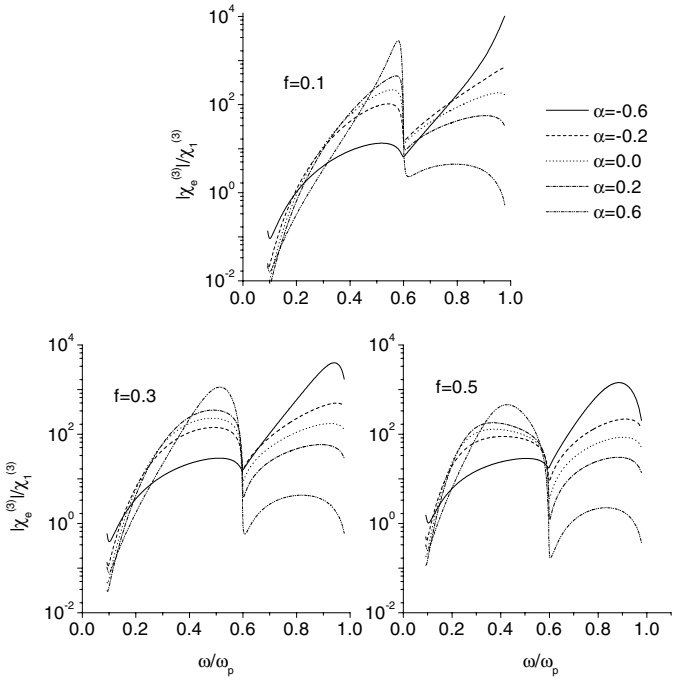

(a)

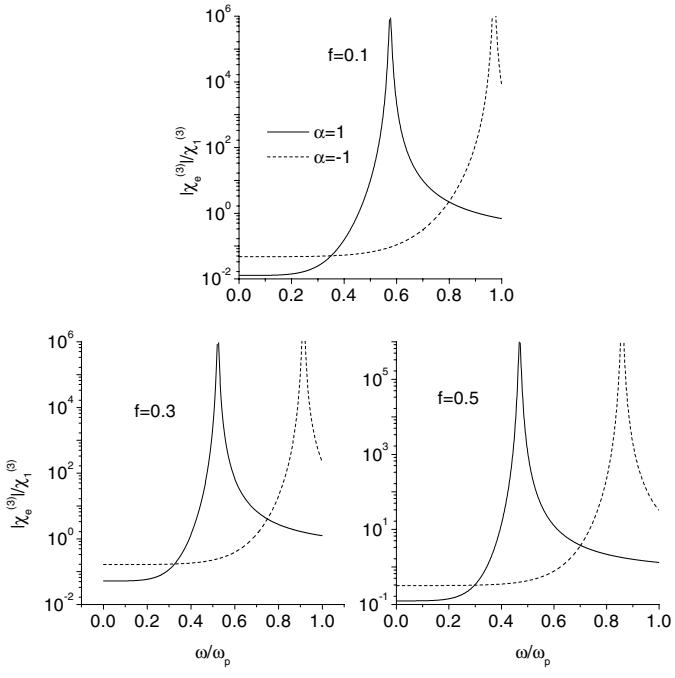

(b)

Figure 3. Similar to figure 2 but for the optical nonlinearity enhancement $|\chi_e^{(3)}|/\chi_1^{(3)}$.

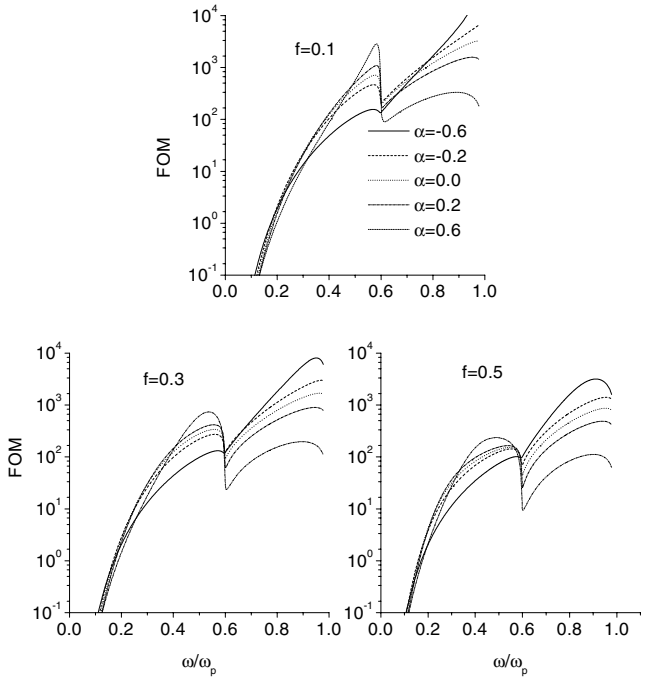

Figure 4. Similar to figure 2(a) but for the figure of merit $|\chi_e^{(3)}|/\mathrm{Im}(\epsilon_e^{(0)})$.

Next, we examine the effect of the distribution parameter α on the optical nonlinearity enhancement $|\chi_e^{(3)}|/\chi_1^{(3)}$, as plotted in figures 3(a) and 3(b). The optical nonlinearity achieves large enhancement in two regions. One is $0.45 \leqslant \omega/\omega_p \leqslant 0.6$ and the other is $0.8 \leqslant \omega/\omega_p \leqslant 1.0$. In the former (latter) region, $|\chi_e^{(3)}/\chi_1^{(3)}$ is increased (decreased) as α increases. With the increase of f, the nonlinearity enhancement band is red-shifted and becomes broad as the dipole interaction increases. More interestingly, the nonlinearity enhancement peak can be separated from the absorption one in the middle-frequency region. This phenomenon is observed for $-1 < \alpha < 0$ in the case of small f such as $f = 0.1$, and becomes more distinct for large f independent of α. Due to this, introducing the shape distribution in this region is beneficial for improving the figure of merit $|\chi_e^{(3)}|/\mathrm{Im}(\epsilon_e^{(0)})$ (FOM). In the large-frequency region, we find the nonlinearity enhancement peak coincides with the optical absorption peak. The coincidence seems to hinder potential applications. However, the magnitude of the optical absorption is more suppressed than that in other regions, still resulting in a large figure of merit, especially for small α.

For practical purposes, the more useful parameter is FOM. In figure 4, we plot FOM $|\chi_e^{(3)}|/\mathrm{Im}(\epsilon_e^{(0)})$ as a function of frequency for various values of α. We can see that FOM is also greatly enhanced in both regions, in accord with the above analysis of the optical nonlinearity. More importantly, the magnitude of FOM can be one or two orders larger than that of previous work [4, 25].

4. Optical nonlinearity in the dilute limit

In section 3, we investigate the optical nonlinearity within the mean-field approximation, As we know, the approximation becomes exact for spherical particles in the dilute limit. However,

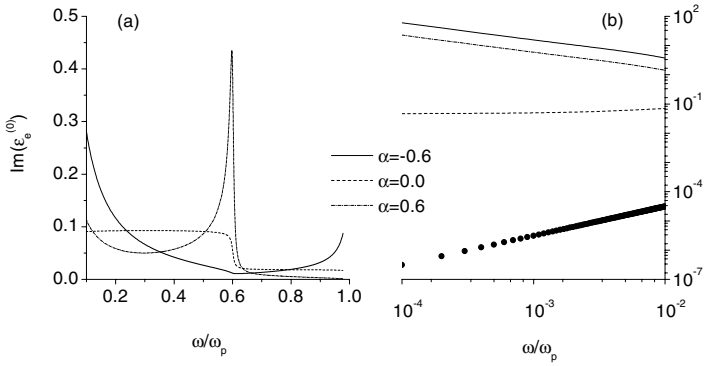

Figure 5. $\mathrm{Im}(\epsilon_e^{(0)})$ as a function of ω/ω_p in the dilute limit $f = 0.01$. Figure 5(b) represents the far-infrared case. The solid circles denote the results for the standard Maxwell–Garnett approximation.

for randomly oriented spheroidal particles, $\langle|\boldsymbol{E}|^2\boldsymbol{E}^2\rangle_{lin,i} \neq \langle|\boldsymbol{E}|^2\rangle\langle\boldsymbol{E}^2\rangle_{lin,i}$, the approximation in equation (21) is rough even in the dilute limit [3]. Here, we derive the formula directly from the definition.

When $f \to 0$, the effective linear response is reduced to

$$\epsilon_e^{(0)} = \epsilon_2^{(0)} + f\beta\left(\epsilon_1^{(0)} - \epsilon_2^{(0)}\right). \tag{23}$$

The expression for the effective optical nonlinearity can be derived from the first equality in equation (21) without any knowledge of the spectral density function,

$$\chi_e^{(3)} = f\chi_1^{(3)}\int_0^1\left[\frac{1}{5}\beta_z^2|\beta_z|^2 + \frac{2}{15}\left(\beta_z^2|\beta_{xy}|^2 + |\beta_z|^2\,\beta_{xy}^2\right) + \frac{8}{15}|\beta_{xy}|^2\beta_{xy}^2\right]P(L_z)\,\mathrm{d}L_z \tag{24}$$

where $\beta_z = \epsilon_2^{(0)}/[\epsilon_2^{(0)} + L_z(\epsilon_1^{(0)} - \epsilon_2^{(0)})]$ and $\beta_{xy} = \epsilon_2^{(0)}/[\epsilon_2^{(0)} + L_{xy}(\epsilon_1^{(0)} - \epsilon_2^{(0)})]$.

Figure 5(a) shows $\mathrm{Im}(\epsilon_e^{(0)})$ as a function of ω/ω_p in the dilute limit such as $f = 0.01$ with equation (23). The results are similar to those in figure 2(a). The optical absorption in the far-infrared region is shown in figure 5(b). By adjusting the distribution parameter α, far-infrared absorption about seven orders of magnitude larger than that predicted by the standard Maxwell–Garnett approximation (MGA) can be achieved [26] (see the curve with solid circles). The magnitude can be comparable to experimental results [27]. However, because we take the shape distribution into account, we do not predict the linear dependence of optical absorption on the frequency ω, which has been observed in the experiment [8] and predicted by the standard MGA.

Figures 6(a) and 6(b) show the optical nonlinearity enhancement with equation (24) and the mean-field approximation. Clearly, the mean-field approximation characterizes the exact results qualitatively. However, as a mean-field approximation, it does underestimate the optical nonlinearity and can not give a sharp enhancement peak at $\omega/\omega_p \approx 0.47$, as shown in figure 6(a).

5. Discussion and conclusions

We have generalized the Maxwell–Garnett type approximation with the 'beta function' distribution of shapes for calculating the effective nonlinear optical properties of metal/dielectric composite materials. Introducing the shape distribution of metallic particles

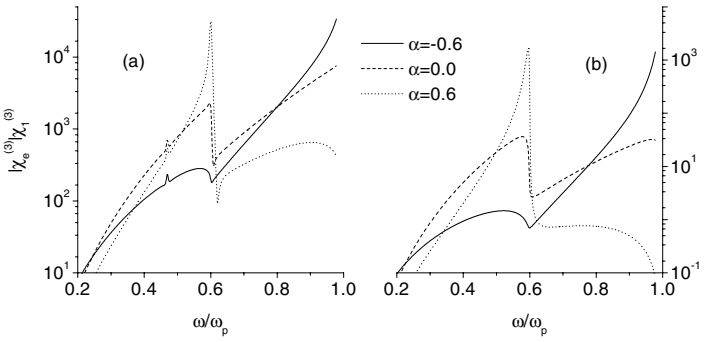

Figure 6. $|\chi_e^{(3)}|/\chi_1^{(3)}$ (a) against ω/ω_p in the dilute limit $f = 0.01$ with equation (24). (b) shows the results with the mean-field approximation.

is helpful to understand the anomalous far-infrared absorption, and make the separation of the optical absorption peak from the nonlinearity enhancement one. Moreover, we present an extra freedom, the distribution parameter α, which is subject to the experimental control, of adjusting the magnitude of optical absorption, optical nonlinearity and figure of merit. In the dilute limit, we derive an exact formula for the effective optical nonlinearity and predict a sharp enhancement peak near the frequency $\omega/\omega_p \approx 0.47$, which is completely neglected within the mean-field approximation.

Experiments and theories [28, 29] suggest that the particular clustering is responsible for the enhancement of the far-infrared absorption. Here we consider an assembly of metal spheroidal particles with a particular distribution function. The surface plasmon resonance peak predicted with the standard MGA and previous work [11] broadens and is red-shifted. We have found anomalous absorption in the far-infrared region, but predicted a deviation from the linear dependence on the frequency. In fact, the anomalous far-infrared absorption mechanism is very complicated, and many factors such as the particle size, coating and shape contribute to it. It seems too simple to attribute this phenomenon only to the shape distribution. However, a shape distribution of small metallic particles may exist under experimental conditions and this may be a key point to explain the anomalous far-infrared absorption behaviour.

Theoretical investigation [5] of the optical nonlinearity of spherical metal/dielectric composites predicts at least two orders larger than experimental reports [12]. By considering the shape distribution, the optical nonlinearity spectrum broadens and the magnitude becomes small, in contrast to the case without shape distribution [5, 11]. Thus it is possible to reduce the discrepancy between the theory and experiment through the shape distribution. In order to compare with experimental results quantitatively, a more realistic distribution function such as the log-normal form should be introduced. We can further extend the model to the system in which both metal particles and the dielectric host are nonlinear. In order to observe strong collective phenomena appearing in the composite media, we should derive the Bruggeman-type effective medium approximation [30, 31] by taking into account the shape distribution.

We propose another way, i.e., by use of shape distribution to realize the separation of linear absorption peak and nonlinearity enhancement one. In order to further promote both the optical nonlinearity and the figure of merit, granular inclusions with a wide distribution of the shape should be prepared in experiments, and the composites may not be studied at the same frequency as the one at which the optical absorption achieves a maximum.

When the metal particles have a shape distribution, the correlation or clustering effects will rise and further affect the optical absorption and optical nonlinearity. The optical nonlinearity

enhancement via short-range correlations has been investigated with numerical simulations [13]. The microstructures with long-range correlations are under investigation and will be discussed elsewhere.

Acknowledgments

LG and ZYL acknowledge the National Natural Science Foundation of China for the financial support under grant No 19774042. LG also acknowledges the Laboratory of Solid State Microstructures, Nanjing University for the financial support under grant No M001511. KWY acknowledges the Research grant Council of Hong Kong SAR government under project No CUHK 4290/98P.

References

[1] Flytzanis C, Hache F, Klein M C, Ricard D and Roussignol P 1991 *Prog. Opt.* **29** 323
[2] See for example 1989 *J. Opt. Soc. Am.* B **6** 1 Special issue on nonlinear optical properties of composite materials ed C M Bowden and J W Haus
[3] Stroud D and Wood V E 1989 *J. Opt. Soc. Am.* B **6** 778
[4] Yuen K P, Law M F, Yu K W and Sheng P 1997 *Phys. Rev.* E **56** R1322
[5] Ma H R, Xiao R F and Sheng P 1998 *J. Opt. Soc. Am.* B **15** 1022
[6] Yuen K P, Law M F, Yu K W and Sheng P 1998 *Opt. Commun.* **148** 197
[7] Gao L and Li Z Y 2000 *J. Appl. Phys.* **87** 1620
[8] Tanner D B, Sievers A J and Buhrman R A 1975 *Phys. Rev.* B **11** 1330
[9] Gao L, Wan J T K , Yu K W and Li Z Y 2000 *J. Appl. Phys.* **88** 1893
[10] Wu Y M, Gao L and Li Z Y 2000 *Phys. Status Solidi* b **220** 997
[11] Gao L, Wan J T K, Yu K W and Li Z Y 2000 *J. Phys.: Condens. Matter* **12** 6825
[12] Liao H B, Xiao R F, Fu J S, Yu P, Wong G K L and Sheng P 1997 *Appl. Phys. Lett.* **70** 1
[13] Law M F, Gu Y and Yu K W 1998 *Phys. Rev.* B **58** 12 536
[14] Bohren C F and Huffman D R 1983 *Absorption and Scattering of Light by Small Particles* (New York: Wiley)
[15] Abramowitz M and Stegun I A 1972 *Handbook of Mathematical functions* (Washington, DC: National Bureau of Standards)
[16] Zakri T, Laurent J P and Vauclin M 1998 *J. Phys. D: Appl. Phys.* **31** 1589
[17] Lichtenecker K 1926 *Phys. Z.* **27** 115
[18] Bergman D J 1978 *Phys. Rep.* **43** 377
[19] Milton G 1980 *J. Appl. Phys.* **52** 5286
[20] Nan C W, Birringer R, Clarke D R and Gleiter H 1997 *J. Appl. Phys.* **81** 6692
[21] Goncharenko A V, Venger E F and Zavadskii S N 1996 *J. Opt. Soc. Am.* B **13** 2392
[22] Goncharenko A V, Lozovski V Z andVenger E F 2000 *Opt. Commun.* **174** 19
[23] Yu K W 1998 *Solid State Commun.* **105** 689
[24] Liao H B, Xiao R F, Fu J S and Wong G K L 1997 *Appl. Phys.* B **65** 673
[25] Yang B F, Zhang C X, Wang Q Q, Zhang Z H and Tian D C 2000 *Opt. Commun.* **183** 307
[26] Maxwell-Garnett J C 1904 *Phil. Trans. R. Soc.* A **203** 385
[27] Kim Y H and Tanner D B 1989 *Phys. Rev.* B **39** 3585
[28] Sen P N and Tanner D B 1982 *Phys. Rev.* B **26** 3582
[29] Curtin W A and Ashcroft N W 1985 *Phys. Rev.* B **31** 3287
[30] Noh T W, Song P H and Sievers A J 1991 *Phys. Rev.* B **44** 5459
[31] Lagarkov A N and Sarychev A K 1996 *Phys. Rev.* B **53** 6318